Transplant Immunology 54 (2019) 38–46

Contents lists available at ScienceDirect

Transplant Immunology

journal homepage: www.elsevier.com/locate/trim

Increased splenic human CD4$^+$:CD8$^+$ T cell ratios, serum human interferon-γ and intestinal human interleukin-17 are associated with clinical graft-versus-host disease in humanized mice

Nicholas J. Geraghty[a,b,c], Lisa Belfiore[a,b,c], Sam R. Adhikary[a,b,c], Stephen I. Alexander[d], Ronald Sluyter[a,b,c], Debbie Watson[a,b,c,*]

[a] School of Chemistry and Molecular Bioscience, University of Wollongong, Wollongong, NSW 2252, Australia
[b] Molecular Horizons, University of Wollongong, Wollongong, NSW 2252, Australia
[c] Illawarra Health and Medical Research Institute, Wollongong, NSW 2252, Australia
[d] Centre for Kidney Research, The Children's Hospital at Westmead, Westmead, NSW, Australia

ARTICLE INFO

Keywords:
Xenogeneic graft-versus-host disease
Humanized mice
Interferon-gamma
Interleukin-17
T lymphocyte

ABSTRACT

Graft-versus-host disease (GVHD) is a frequent complication following allogeneic hematopoietic stem cell transplantation (HSCT) with current therapies limited to general immunosuppression. Humanized mouse models of GVHD are emerging as valuable intermediaries to allow translation of findings from allogeneic mouse models to humans to prevent and treat this disease, but such models require further characterization. In this study, humanized mice were generated by injecting immunodeficient non-obese diabetic severe combined immunodeficiency interleukin (IL)-2 receptor γ common chain null (NSG) mice with human peripheral blood mononuclear cells (hPBMCs). Clinical GVHD development was assessed using established scoring criteria (weight loss, posture, activity, fur texture and skin integrity). Differences between humanized NSG mice that developed clinical or subclinical GVHD were then compared. Both groups of mice demonstrated similar frequencies of human leukocyte engraftment. In contrast, mice that developed clinical GVHD demonstrated increased histological damage compared to mice with subclinical GVHD. Furthermore, mice with clinical GVHD exhibited increases in the splenic human CD4$^+$:CD8$^+$ T cell ratio, serum human interferon (IFN)-γ and intestinal human IL-17 expression compared to mice with subclinical GVHD. These cellular and molecular changes could be used as potential markers of disease progression in this preclinical model. This study also provides further insights into GVHD development which may be relevant to human HSCT recipients.

1. Introduction

Allogeneic hematopoietic stem cell transplantation (HSCT) is a curative therapy for haematological malignancies and other blood disorders. However, graft-versus-host disease (GVHD) occurs in approximately half of the HSCTs conducted annually [1] and leads to a mortality rate of approximately 20% in these patients [2]. GVHD emerges when effector donor T cells mount an immune response against host tissues [3]. GVHD is characterized by three stages. The first stage is release of danger signals from cells damaged by the underlying disease and/or conditioning regimes, followed by CD4$^+$ T cell activation by antigen presenting cells resulting in cytokine release, and finally CD4$^+$ and CD8$^+$ T cell-mediated inflammatory damage [4,5]. This damage can be propagated by the "cytokine storm" in the latter stage, wherein Th1 and Th17 cells release pro-inflammatory cytokines such as interferon (IFN)-γ [4,5] and interleukin (IL)-17 [6,7], respectively, perpetuating a feed forward loop of inflammation. Conversely, regulatory T (Treg) cells can modulate effector T cells to reduce T cell-mediated inflammatory damage in GVHD [8]. Current therapies for GVHD are limited, with the standard therapy being general immunosuppression

Abbreviations: APC, Allophycocyanin; ANOVA, one-way analysis of variance; FITC, fluorescein isothiocyanate; FoxP3, forkhead box P3; GVHD, graft-versus-host disease; h, human; hPBMCs, human peripheral blood mononuclear cells; HSCT, hematopoietic stem cell transplantation; IFN, interferon; IL, interleukin; mAb, monoclonal antibody; m, murine; MST, median survival time; NSG, non-obese diabetic severe combined immunodeficiency interleukin-2 receptor γ common chain null; PE, R-phycoerythrin; Per-CP, peridinin chlorophyll protein; qPCR, quantitative real-time PCR; TNF-α, tumour necrosis factor alpha; Treg, regulatory T cell

* Correspondence to: School of Chemistry and Molecular Bioscience, University of Wollongong, Illawarra Health and Medical Research Institute, Northfields Avenue, Wollongong, NSW 2522, Australia.
E-mail address: dwatson@uow.edu.au (D. Watson).

https://doi.org/10.1016/j.trim.2019.02.003
Received 22 May 2018; Received in revised form 7 February 2019; Accepted 7 February 2019
Available online 08 February 2019
0966-3274/

achieved through steroids, leaving patients susceptible to subsequent infections and/or disease relapse [9]. Therefore, greater understanding of the mechanisms important in GVHD and elucidation of new therapies is essential to improve outcomes in HSCT patients and prevent GVHD.

Current studies into potential therapeutics for GVHD are investigated in allogeneic mouse models before translation to the clinic. However, potentially due to large species differences between humans and mice, therapies that delay or prevent GVHD in allogeneic mouse models often do not translate to the clinic. To address this, previous studies have developed a range of preclinical "humanized" mouse models [10]. The most commonly used of these models is the humanized immunodeficient non-obese diabetic severe combined immunodeficiency IL-2 receptor γ common chain null (NSG) mouse, developed by Shultz et al. [11] wherein mice readily engraft human peripheral blood mononuclear cells (hPBMCs) due to three defects. First, the *Scid* mutation prevents V(D)J recombination to impair B and T cell development [12]. Second, deletion of the *Il2rg* gene results in absence of natural killer (NK) cells. Third, a polymorphism in the *Sirpa* gene, present due to backcrossing onto a NOD background, promotes phagocytic tolerance of xenogeneic leukocytes [13]. Human T cells recognize major histocompatibility complex (MHC) class I and II of NSG mice to cause GVHD in this humanized mouse model [14], demonstrating that human T cell responses can be investigated in vivo to better understand this disease in a preclinical setting.

The humanized NSG model of GVHD is emerging as a valuable intermediate to allow translation of findings identified in allogeneic mouse models to human clinical trials. For example, based on an earlier study in an allogeneic mouse model of GVHD [15], King, et al. [14] demonstrated tumour necrosis factor (TNF)-α blockade could reduce GVHD severity in this humanized mouse model, and etanercept, an anti-TNF-α monoclonal antibody (mAb) has subsequently shown efficacy in clinical trials [16]. More recently, Burger et al. [17] demonstrated an anti-CCR5 mAb (PRO 140) could reduce GVHD in humanized NSG mice, with this mAb now being investigated in clinical trials [18]. Finally, the discovery of Treg cells, and their therapeutic potential in GVHD has progressed from allogeneic mouse models [8], to humanized NSG models [19,20], and finally to clinical trials [21]. Moreover, this model has helped elucidate the action of post-transplant cyclophosphamide on Treg cells in GVHD development [22]. Therefore, the humanized NSG model offers a valid preclinical model to test therapies for translation to the clinic. Although this mouse model has offered numerous advancements, the characterization of GVHD in these mice has not been adequately described.

2. Objective

The current study aimed to investigate the characteristics of GVHD that were observed in humanized NSG mice injected with human PBMCs that developed clinical disease compared to those mice that displayed subclinical GVHD. This study demonstrated that all humanized NSG mice had similar engraftment of human leukocytes, which were predominantly T cells. In contrast, humanized NSG mice with clinical GVHD demonstrated greater splenic $CD4^+$:$CD8^+$ T cells ratios, serum human IFN-γ concentrations and intestinal human IL-17 expression than humanized mice with subclinical GVHD. These cellular and molecular changes could potentially be used as biomarkers of disease progression in this preclinical model and provide insights into GVHD development which may be applicable to human HSCT recipients.

3. Materials and methods

3.1. Antibodies for flow cytometry

Fluorescein isothiocyanate (FITC)-conjugated mouse anti-hCD4 (clone: RPA-T4), and mouse anti-hCD45 (clone: HI30); R-phycoerythrin (PE)-conjugated mouse anti-hCD3 (clone: UCHT1) and mouse anti-hCD8 (clone: RPA-T8); peridinin chlorophyll protein (PerCP)-Cy5.5 conjugated mouse anti-hCD4 (clone: L200) and rat anti-mCD45 (clone: 30-F11); and allophycocyanin (APC)-conjugated mouse anti-hCD3 (clone: UCHT1) and mouse anti-hCD19 (clone: HIB19) mAb were obtained from BD (San Jose, CA, USA).

3.2. Mice

All mouse experiments were conducted in accordance with approval by the Animal Ethics Committee, University of Wollongong (Wollongong, Australia). Female NSG mice, originally obtained from The Jackson Laboratory (Bar Harbor, ME, USA), were bred at the Westmead Animal Research Facility (Westmead, Australia) or Australian BioResources (Moss Vale, Australia). NSG mice, obtained at 6–10 weeks of age, were housed in filter top cages in Tecniplast (Buggugiate, Italy) isolation cabinets, and provided with autoclaved food and water, ad libitum. Mice were allowed to acclimatize for one week prior to injection.

3.3. Isolation of human PBMCs

All experiments with human blood were conducted in accordance with approval by the Human Ethics Committee, University of Wollongong. Peripheral blood was collected by venepuncture into VACUETTE® lithium heparin tubes (Greiner Bio-One; Frickenhausen, Germany). Whole blood, diluted with an equal volume of sterile phosphate buffered saline (PBS) (Thermo Fisher Scientific, Waltham, USA), was underlaid with Ficoll-Paque PLUS (GE Healthcare; Uppsala, Sweden) and centrifuged (560 × *g* for 30 min). hPBMCs were collected and washed with PBS (430 ×*g* for 5 min) and resuspended in PBS.

3.4. Humanized NSG mouse model of GVHD

NSG mice were injected intra-peritoneally (i.p) with 10×10^6 hPBMCs (from the same donor) in 100 µL sterile PBS (hPBMC group) or with 100 µL sterile PBS alone (control group) (day 0). Mice were checked for engraftment of hPBMCs at 3 weeks post-injection by immunophenotyping tail blood. Mice were monitored up to week 8 for signs of GVHD using a scoring system [23] giving a total clinical score

Table 1
Scoring system for clinical GVHD.

Grade	0	1	2
Weight loss[a]	< 5%	5% to 10%	> 10%
Posture	Normal	Hunching noted only at rest	Severe hunching
Activity	Normal	Mild to moderately decreased	Stationary unless stimulated
Fur texture	Normal	Mild to moderate ruffling	Severe ruffling
Skin Integrity	Normal	Scaling of paws/tail	Obvious areas of involved skin

Mice are assigned a score out of 2 for each of the criterion outlined to give a total score of 10 (as previously described [23]). Humanized mice with clinical score < 3 were defined as subclinical GVHD, and mice with a clinical score ≥ 3 were defined as clinical GVHD.

[a] Percent of starting weight (day 0).

out of 10 (Table 1). Mice were euthanized at end-point either 8 weeks post-injection or earlier if exhibiting a clinical score of ≥8 or a weight loss of ≥10%, according to the approved animal ethics protocol.

3.5. Immunophenotyping by flow cytometry

Tail blood (20–30 μL) was collected 3 weeks post-hPBMC injection into 200 μL of citrate solution (Sigma-Aldrich), diluted with PBS and centrifuged (500 ×*g* for 5 min). Spleens from euthanized mice at end-point were mechanically dissociated, filtered through 70 μm nylon filters (Falcon Biosciences, New York, NY, USA) and centrifuged (300 ×*g* for 5 min). Blood and spleen cells were incubated with ammonium chloride potassium (ACK) lysis buffer (150 mM NH_4Cl, 1 mM $KHCO_3$, 0.1 mM Na_2CO_3, pH 7.3) for 5 min and washed in PBS (300 × g for 5 min). Cells were then washed in PBS containing 2% foetal bovine serum (300 × g for 3 min), and incubated for 30 min with fluorochrome-conjugated mAb, including respective isotype controls. Cells were washed with PBS (300 × g for 3 min) and data was collected using a BD LSRII Flow Cytometer (using band pass filters 515/20 for FITC, 575/26 for PE, 675/40 for PerCP-Cy5.5, and 660/20 for APC). The relative percentages of cells were analyzed using FlowJo software v8.7.1 (TreeStar Inc., Ashland, OR, USA).

3.6. Histological analysis

Tissues from euthanized mice at end-point were incubated overnight in neutral buffered (10%) formalin (Sigma-Aldrich). Fixed tissues were removed, coated in paraffin, sectioned (5 μm) and stained with haematoxylin and eosin (POCD; Artarmon, Australia). Histological changes were assessed using a Leica (Wetzlar, Germany) DMRB microscope and Leica Application Software version 4.3.

3.7. RNA isolation and cDNA synthesis

Tissues from euthanized mice at end-point or freshly isolated hPBMCs were stored in RNAlater (Sigma-Aldrich) at −20 °C. RNA was isolated using TRIzol reagent (Thermo Fisher Scientific) as per the manufacturer's instructions. Isolated RNA was immediately converted to complementary DNA (cDNA), using the qScript cDNA Synthesis Kit (Quanta Biosciences, Beverly, MA, USA) as per the manufacturer's instructions, and RNA stored at −80 °C. cDNA was checked by PCR amplification of the house keeping gene glyceraldehyde 3-phosphate dehydrogenase (Invitrogen, Carlsbad, CA, USA) for 35 cycles (95 °C for 1 min, 55 °C for 1 min, and 72 °C for 1 min) and a holding temperature of 4 °C. Purity and size of amplicons were confirmed by 2% agarose gel electrophoresis.

3.8. Quantitative real-time PCR

Quantitative real-time PCR (qPCR) reactions of cDNA samples were using TaqMan Universal Master Mix II (Thermo Fisher Scientific) according to the manufacturer's instructions, with VIC-labelled human hypoxanthine phosphoribosyl transferase 1 (Hs99999909_m1) and FAM-labelled hIFN-γ (Hs00989291_m1), hIL-17 (Hs00936345_m1) and hFoxP3 (Hs01085834_m1) primers (Thermo Fisher Scientific). qPCR cycles consisted of two initial steps of 50 °C for 2 min, and 95 °C for 10 min and 40 cycles of 95 °C for 15 s, and 60 °C for 1 min. Reactions were conducted in triplicate using a Roche Diagnostics (Indianapolis, IN, USA) LightCycler 480, and analysis was conducted using LightCycler480 software v1.5.1. Human gene expression is shown relative to expression in cDNA from freshly isolated donor hPBMCs.

3.9. ELISA

Blood, collected via cardiac puncture from euthanized mice at end-point, was incubated for 1 h at RT and centrifuged (1700 ×*g* for 10 min). Supernatants were re-centrifuged (1700 ×*g* for 10 min) and sera stored at −80 °C. Serum cytokine concentrations were measured using a hIFN-γ Ready-Set-Go! ELISA Kit (eBioscience, San Diego, CA, USA) as per the manufacturer's instructions. Absorbances (450 and 570 nm) were measured using a SpectraMax Plus 384 (Molecular Devices, Sunnyvale, CA, USA).

3.10. Statistical analysis

Data is given as mean ± standard error of the mean (SEM). Statistical differences were calculated using Student's *t*-test for single comparisons or one-way analysis of variance (ANOVA) with Tukey's post-hoc test for multiple comparisons. Weight and clinical score were analyzed using a repeated measures two-way ANOVA with Tukey's post-hoc test for multiple comparisons. Median survival times (MST) were compared using the log-rank (Mantel-Cox) test. Proportions of mice sacrificed prior to week 8 (mortality rates) were compared using Fisher's Exact test. All statistical analyses and graphs were generated using GraphPad Prism 5 for PC (GraphPad Software, La Jolla, CA, USA). $P < 0.05$ was considered significant for all tests.

4. Results

4.1. Clinical GVHD development varies in humanized NSG mice

NSG mice, injected i.p. with either saline (control) or hPBMCs, were monitored for physical manifestations of GVHD over 8 weeks. After 4 weeks, humanized NSG mice with GVHD started to exhibit clinical

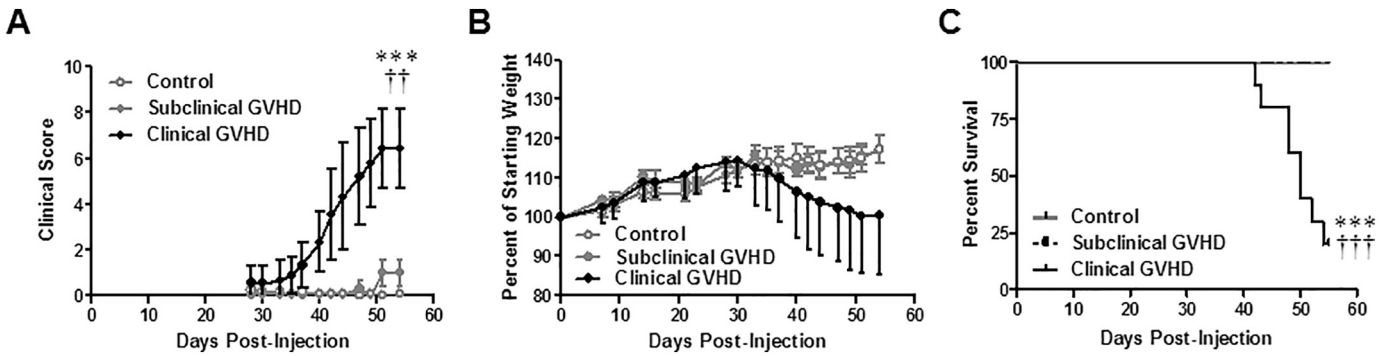

Fig. 1. Clinical GVHD development varies in humanized mice.
(A-C) NSG mice were injected i.p. with PBS (control) ($n = 6$) or 10×10^6 hPBMCs in PBS ($n = 13$) and monitored for GVHD over 8 weeks. NSG mice were monitored for (A) clinical score, (B) weight loss and (C) survival. Humanized mice with subclinical GVHD ($n = 3$) were defined as having a clinical score < 3 and mice with clinical GVHD ($n = 10$) were defined as having a clinical score ≥ 3. Data represents (A, B) group means ± SEM, or (C) percent survival from two experiments using a single hPBMC donor; *** $P < 0.0001$ compared to control mice, †† $P < 0.01$ and ††† $P < .0001$ compared to mice with subclinical GVHD.

signs of disease (Fig. 1A). By end-point it became apparent that hPBMC-injected mice segregated into one of two groups based on clinical score (Table 1); one group with scores ≥3 (clinical GVHD) and another group with scores < 3 (subclinical GVHD) (Fig. 1A). Mice with clinical scores ≥3 exhibited weight loss, reduced activity, postural changes (hunching) and fur ruffling, with skin involvement in some mice, whilst mice with clinical scores < 3 was solely attributed to fur ruffling and/or postural changes (data not shown). The mean clinical score over the course of the experiment in humanized mice with clinical GVHD was greater than both control mice and mice with subclinical GVHD ($P < 0.0001$ and $P = 0.0010$, respectively) (Fig. 1A). Weight loss alone is indicative of GVHD development [24]. Notably, control mice and humanized mice with subclinical GVHD continued to gain weight over the entire 8 weeks, however, humanized mice with clinical GVHD started to lose weight after 4 weeks (Fig. 1B). Although this difference was obvious after 4 weeks, the weight loss was not statistically significant between groups ($P = 0.2871$). Humanized mice with clinical GVHD had a MST of 50 days, which was significantly worse than control mice ($P < 0.0001$) and humanized mice with subclinical GVHD ($P < 0.0001$) where all mice survived for 8 weeks (Fig. 1C). Humanized mice with clinical GVHD exhibited an 80% mortality rate over 8 weeks, which was significantly greater than control mice ($P < 0.0001$) or humanized mice with subclinical GVHD ($P = 0.0350$) (Fig. 1C).

4.2. Increased histological damage and leukocyte infiltration is associated with clinical GVHD

GVHD targets the liver, gastro-intestinal tract and skin in humanized NSG mice [14,23], similar to humans [5]. To compare control NSG mice and humanized NSG mice with clinical or subclinical GVHD, histological analyses of target tissues were conducted, as well as spleens to examine evidence of engraftment at end-point. As expected, control mice demonstrated normal architecture and minimal presence of leukocytes in spleens, livers, small intestines and skin (Fig. 2). Both humanized NSG mice with subclinical or clinical GVHD demonstrated leukocyte infiltration in spleens (Fig. 2), consistent with engraftment of hPBMCs. However, mice with subclinical GVHD demonstrated leukocyte infiltration and minor apoptosis in the liver, whilst mice with clinical GVHD demonstrated greater leukocyte infiltration and greater apoptosis compared to both control mice and humanized mice with subclinical GVHD (Fig. 2). Humanized mice with subclinical GVHD demonstrated leukocyte infiltration and minor damage to enterocytes and occasional crypt epithelial cell apoptosis in the small intestine (Fig. 2). Humanized mice with clinical GVHD demonstrated increased leukocyte infiltration and structural damage including rounding of villi, enterocyte loss and crypt epithelial cell apoptosis in the small intestine compared to mice with subclinical GVHD (Fig. 2). Humanized mice with subclinical GVHD demonstrated similar intact architecture and leukocyte infiltration to control mice in the skin, except for separation at the dermal subcutaneous boundary in the former group (Fig. 2). The skin of humanized mice with clinical GVHD demonstrated leukocyte infiltration, epidermal thickening, basal epithelial cell apoptosis and dermal-subcutaneous boundary separation (Fig. 2).

4.3. Similar engraftment of hPBMCs in mice with subclinical and clinical GVHD

To confirm that NSG mice injected with hPBMCs engrafted human leukocytes, blood was collected at 3 weeks post-injection and spleens were collected at end-point and analyzed by flow cytometry. Blood (Fig. 3A–D) and spleens (Fig. 3E–J) revealed both murine (m) and human (h) $CD45^+$ cells in hPBMC-injected mice (Fig. 3A, E). As expected, control mice demonstrated $mCD45^+$ but no $hCD45^+$ cells in the blood and spleen (Fig. 1B, F).

The frequency of $hCD45^+$ leukocytes were calculated as a percentage of total $hCD45^+$ and $mCD45^+$ cells. In the blood, mean $hCD45^+$ engraftment was similar between mice with subclinical GVHD (15.1 ± 2.2%, $n = 3$) and mice with clinical GVHD (15.3 ± 3.2, $n = 10$) ($P = 0.9737$) (Fig. 3B). $hCD45^+$ cells in the blood of hPBMC-injected mice were then analyzed for the presence of $hCD3^+$ (human T cells) and $hCD19^+$ cells (human B cells) (Fig. 3A). NSG mice injected with hPBMCs showed the majority of engrafted human leukocytes were T cells. The mean percentage of T cells in blood did not differ between mice with subclinical GVHD (99.1 ± 0.1%, $n = 3$) or clinical GVHD (98.1 ± 0.4%, $n = 10$) ($P = 0.1500$) (Fig. 3C). The remaining cells in the blood were $hCD3^-$ and $hCD19^-$, the frequencies of which did not differ between mice with subclinical GVHD (0.8 ± 0.1%, $n = 3$) or clinical GVHD (1.8 ± 0.4%, $n = 10$) ($P = 0.1869$) (Fig. 3D).

Similar to blood, mean $hCD45^+$ engraftment in spleens at end-point was similar between mice with subclinical GVHD (90.9 ± 1.7%, $n = 3$) and clinical GVHD (87.7 ± 2.9%, $n = 10$, respectively) ($P = 0.5880$) (Fig. 3F). Moreover, NSG mice injected with hPBMCs showed the majority of engrafted human leukocytes in spleens were T cells. The mean percentage of T cells in spleens did not differ between mice with subclinical GVHD (97.8 ± 0.5%, $n = 3$) or clinical GVHD (98.4 ± 0.2%, $n = 10$) ($P = 0.1942$) (Fig. 3G). The remaining cells in spleens were $hCD3^-$ and $hCD19^-$, the frequencies of which did not differ between mice with subclinical GVHD (2.2 ± 0.5%, $n = 3$) or clinical GVHD (1.6 ± 0.2%, $n = 10$) ($P = 0.1942$) (Fig. 3H).

Further analysis of the splenic human T cells ($hCD3^+$ $hCD19^-$ cells) (Fig. 3E) revealed that mice with clinical GVHD demonstrated significantly greater proportions of $hCD4^+$ T cell engraftment (85.1 ± 2.0%, $n = 10$) than mice with subclinical GVHD (45.5 ± 8.4%, $n = 3$) ($P < 0.0001$) (Fig. 3I). Conversely, mice with clinical GVHD demonstrated significantly lower proportions of $hCD8^+$ T cell engraftment (12.8 ± 1.7%, $n = 10$) than mice with subclinical GVHD (50.9 ± 8.8%, $n = 3$) ($P < 0.0001$) (Fig. 3I). Moreover, mice with clinical but not subclinical GVHD demonstrated a significantly greater proportion of $hCD4^+$ than $hCD8^+$ T cells ($P < 0.0001$), resulting in higher splenic $hCD4^+$:$hCD8^+$ T cell ratios (8.5 ± 1.7, $n = 10$) than mice with subclinical GVHD (1.0 ± 0.3, $n = 3$) ($P = 0.0418$) (Fig. 3J).

4.4. Increased serum human IFN-γ is associated with clinical GVHD

IFN-γ has been implicated in GVHD pathogenesis [25] and correlates to worse disease in mice with allogeneic GVHD [26]. Therefore, to determine if humanized NSG mice with GVHD demonstrate changes in hIFN-γ, mRNA expression and serum concentrations of this cytokine were analyzed by qPCR and ELISA at end-point, respectively. There was a 3-fold increase in relative hIFN-γ expression in spleens from mice with clinical GVHD (0.7 ± 0.2, $n = 3$) compared to mice with subclinical GVHD (0.2 ± 0.1, $n = 3$) ($P = 0.0880$) (Fig. 4A). There was also a 1.5-fold increase in relative hIFN-γ expression in livers from mice with clinical GVHD (0.9 ± 0.1, $n = 3$) compared to mice with subclinical GVHD (0.6 ± 0.3, $n = 3$) ($P = 0.2576$) (Fig. 4B). However, small intestines from humanized mice with subclinical GVHD or clinical GVHD demonstrated similar relative hIFN-γ expression (0.7 ± 0.3 vs 0.9 ± 0.1, $n = 3$) ($P = 0.5907$) (Fig. 4C). Notably, mice with clinical GVHD demonstrated significantly increased serum human IFN-γ concentrations (42.9 ± 2.7 ng/mL, $n = 5$) compared to mice with subclinical GVHD (25.0 ± 5.5 ng/mL, $n = 3$) ($P = 0.0155$) (Fig. 4D).

4.5. Increased intestinal hIL-17 is associated with clinical GVHD

IL-17 exacerbates GVHD in allogeneic mouse models of this disease [27,28] and in HSCT patients [29]. Whilst, FoxP3 Treg cells exert anti-inflammatory effects in allogeneic [8] and humanized mouse models [30], as well as in humans [31] to prevent GVHD. To further explore potential immunological differences between humanized NSG mice with subclinical or clinical GVHD, relative mRNA expression of hIL-17

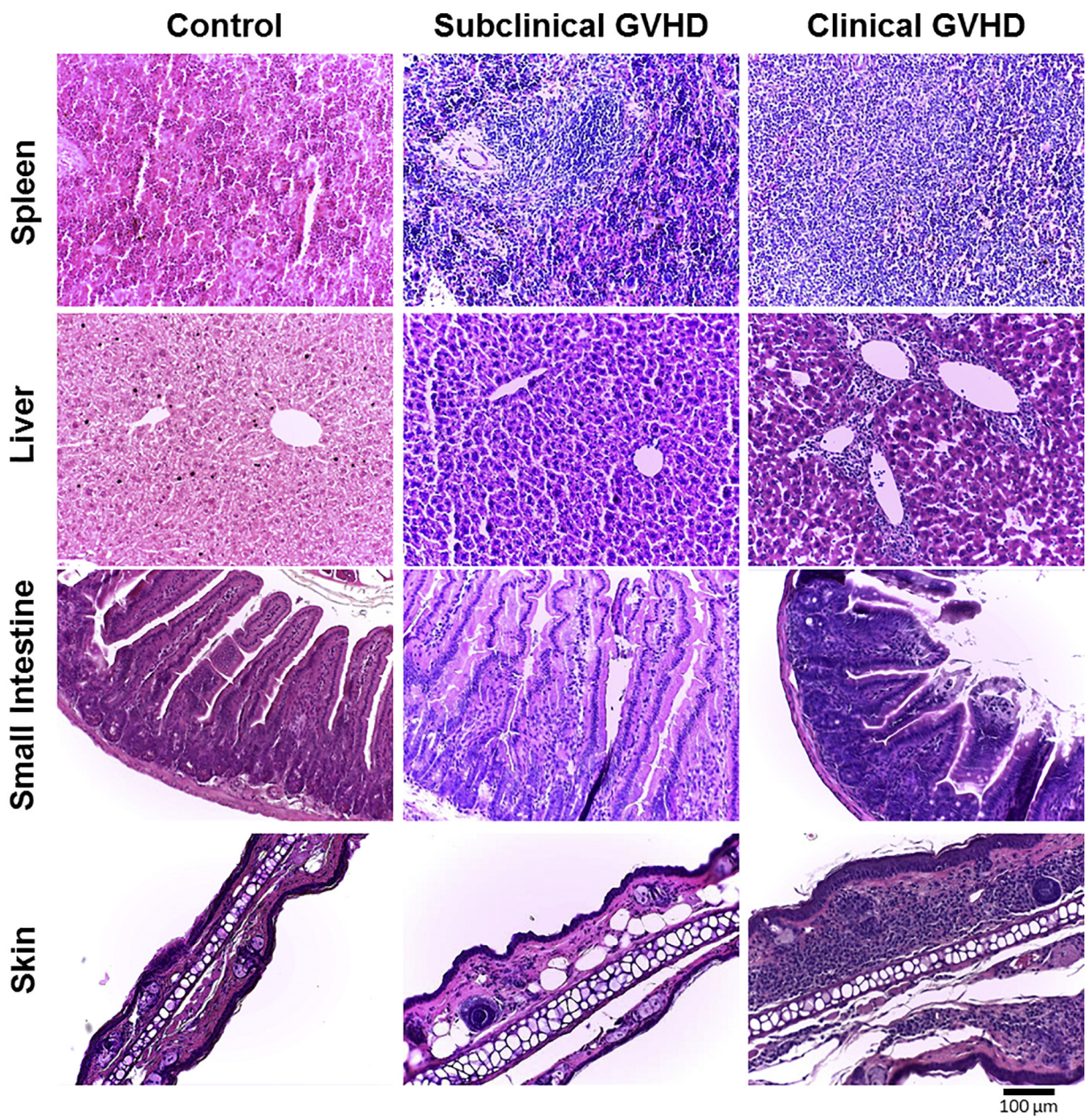

Fig. 2. Increased histological damage and leukocyte infiltration is associated with clinical GVHD.
Tissue sections (spleen, liver, small intestine and skin) from control mice (left panels) or hPBMC-injected mice with subclinical GVHD (middle panels) or clinical GVHD (right panels) at end-point were stained with haematoxylin and eosin, and images captured by microscopy. Each image is representative of three mice per group from two experiments using a single hPBMC donor; bar represents 100 µm.

and hFoxP3 in the spleen, liver and small intestine was assessed by qPCR at end-point.

Relative splenic hIL-17 expression in mice with clinical GVHD (0.5 ± 0.2, $n = 3$) was 40% lower compared to mice with subclinical GVHD (1.3 ± 0.5, $n = 3$) ($P = 0.2505$) (Fig. 5A). However, hepatic hIL-17 expression was similar between mice with clinical GVHD (1.5 ± 0.9, $n = 3$) and subclinical GVHD (1.2 ± 0.2, $n = 3$) ($P = 0.7717$) (Fig. 5B). Notably, intestinal hIL-17 expression was evident in mice with clinical GVHD (1.8 ± 0.4, $n = 3$) but was absent in mice with subclinical GVHD (0.0 ± 0.0, $n = 3$) (Fig. 5C).

Relative splenic hFoxP3 expression was similar in humanized mice with subclinical GVHD (1.2 ± 1, $n = 3$) or clinical GVHD (0.6 ± 0.2, $n = 3$) ($P = 0.5669$) (Fig. 5D). Relative hepatic hFoxP3 expression was also similar in humanized mice with subclinical GVHD (1.3 ± 0.5, $n = 3$) or clinical GVHD (0.6 ± 0.2 and 2.0 ± 0.8, $n = 3$) ($P = 0.4838$) (Fig. 5E). However, there was a 17-fold but variable increase in intestinal hFoxP3 expression in mice with clinical GVHD (0.5 ± 0.3, $n = 3$) compared to mice with subclinical GVHD (0.03 ± 0.01, $n = 3$) ($P = 0.2020$) (Fig. 5F).

5. Discussion

Humanized NSG mouse models of GVHD are used as preclinical models to test potential therapeutics [10], however these models have not been fully characterized. The current study compared humanized NSG mice with subclinical and clinical GVHD, which paralleled the degree of histological disease. Notably, mice with clinical GVHD exhibited greater splenic $hCD4^+$:$hCD8^+$ T cell ratios, serum hIFN-γ concentrations and intestinal hIL-17 expression than mice with subclinical GVHD. However, it should be noted that in two other

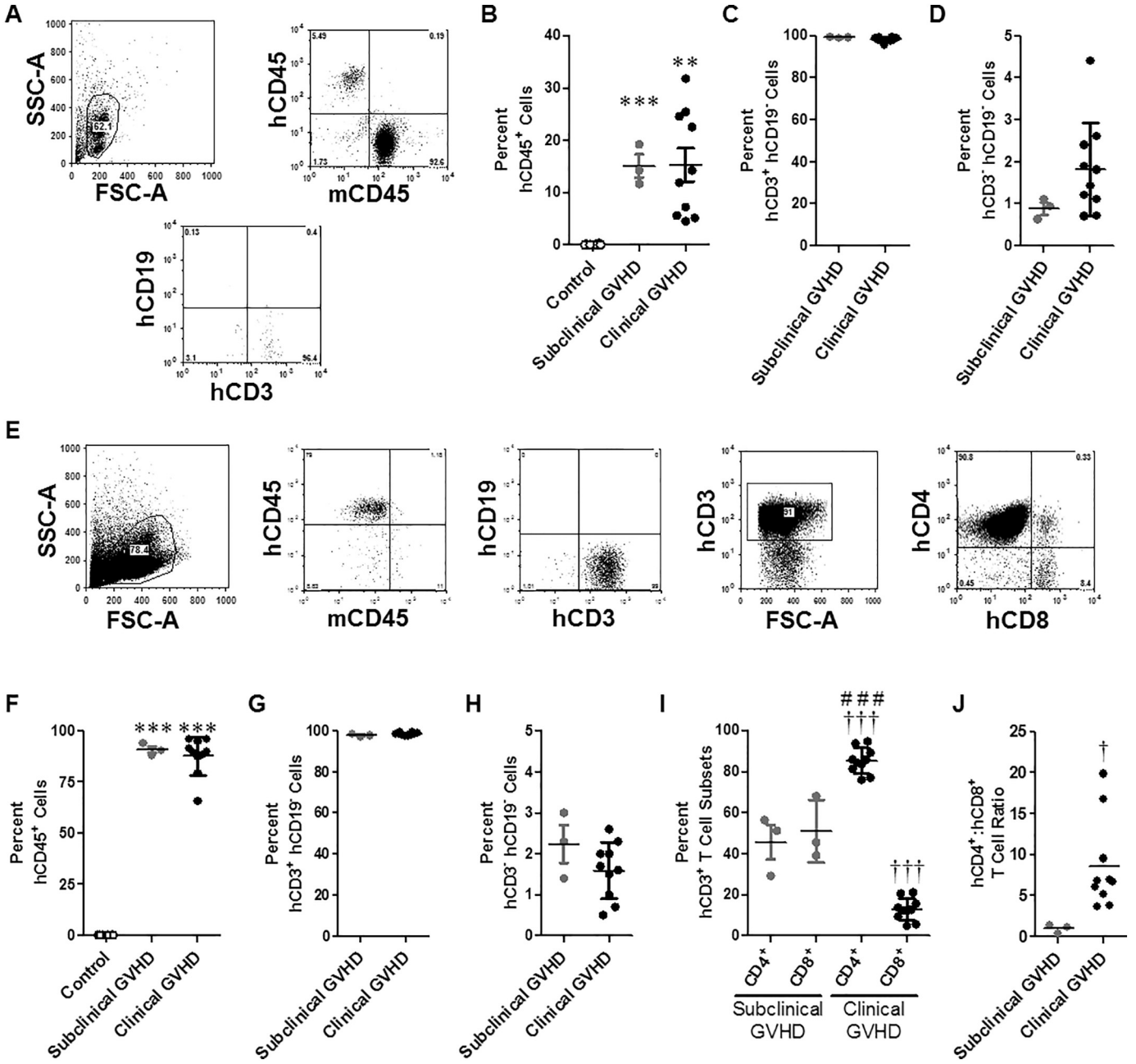

Fig. 3. Humanized mice with clinical GVHD exhibit increased human $CD4^+$:$CD8^+$ T cell ratios.
(A-D) Blood (3 weeks post-hPBMC injection) and (*E*-F) spleens (end-point) from mice were analyzed by flow cytometry. Representative gates and quadrant regions are shown (A, E). (B-F) $hCD45^+$ leukocytes ($hCD45^+$ $mCD45^-$) are expressed as a percentage of total leukocytes ($hCD45^+$ $mCD45^-$ + $hCD45^-$ $mCD45^+$). (C, G) $hCD3^+$ $hCD19^-$ cells and (D, H) $hCD3^-$ $hCD19^-$ cells are expressed as a percentage of $hCD45^+$ leukocytes. $hCD4^+$ and $hCD8^+$ T cells are expressed as a percentage of $hCD3^+$ T cells and (J) used to determine $hCD4^+$:$hCD8^+$ T cell ratios. (B-D, C-J) Data represents group means ± SEM; symbols represent individual mice from two experiments using a single hPBMC donor; ** $P < 0.01$, *** $P < 0.0001$ compared to control mice; † $P < 0.05$, ††† $P < 0.0001$ compared to corresponding cells in mice with subclinical GVHD; $^{\#\#\#}$ $P < 0.0001$ compared to corresponding $CD8^+$ T cells.

independent experiments with hPBMCs from two different donors all NSG mice developed clinical GVHD (data not shown).

Humanized mice with a clinical score < 3 were defined as having subclinical GVHD, and only showed signs of mild to moderate fur ruffling and/or hunching only at rest. These two criteria compared to the other three criteria used are relatively subjective [32], and thus may be attributed to events such as being recently awoken rather than GVHD per se. Analysis of liver, small intestine and skin revealed that all humanized NSG mice had histological evidence of GVHD (leukocyte infiltration, apoptosis and/or tissue damage). Although the leukocyte infiltrates in these tissues were not assessed, previous studies have confirmed infiltrates comprise $hCD45^+$ leukocytes [14] predominantly $hCD3^+$ T cells [33,34], comprising $hCD4^+$ and $hCD8^+$ T cells [35]. Of note, histological evidence of GVHD was more apparent in humanized mice with clinical GVHD compared to those with subclinical GVHD. The reduced histological GVHD in mice with subclinical GVHD is similar to that observed in the livers [33,34,36,37] and small intestine [33,38] of humanized mice following various treatments to prevent GVHD. To this end, the current study provided the opportunity to examine differences in humanized mice with subclinical versus clinical GVHD, and to determine factors that correspond with clinical GVHD development. However, the lung and bone marrow are also affected in

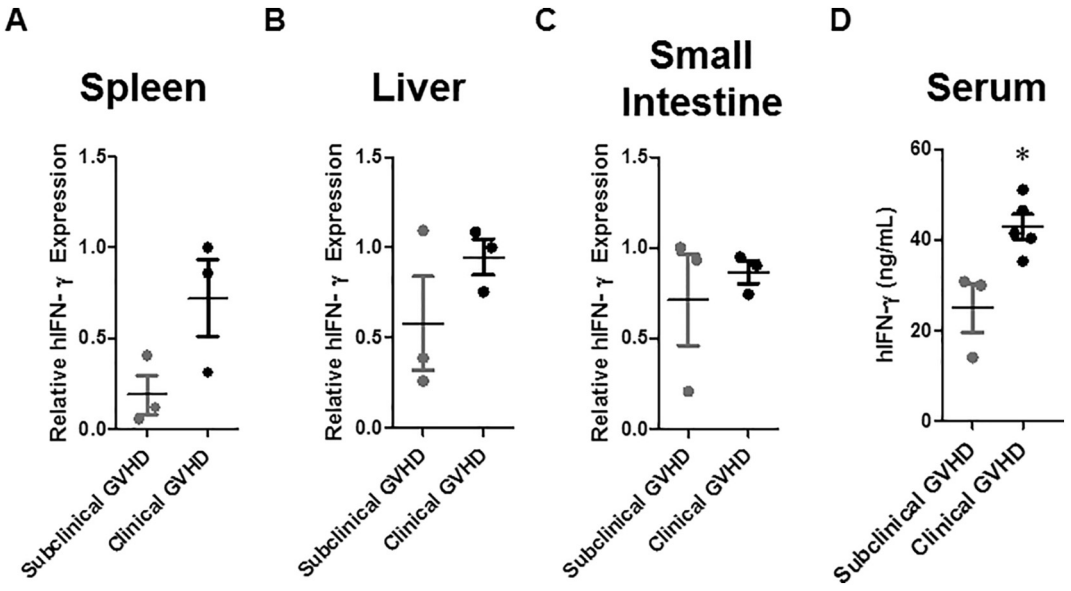

Fig. 4. Humanized mice with clinical GVHD demonstrate increased serum hIFN-γ concentrations.
The relative expression of hIFN-γ in (A) spleens, (B) livers and (C) small intestines from mice with subclinical and clinical GVHD at end-point were examined by qPCR. Data represents group means ± SEM (n = 3 per group); symbols represent individual mice from two experiments using a single hPBMC donor. (D) Serum hIFN-γ concentrations were analyzed by ELISA. Data represents group means ± SEM (subclinical GVHD n = 3, clinical GVHD n = 5); * $P < 0.05$ compared to mice with subclinical GVHD.

the humanized NSG mouse model of GVHD [14,35]. Thus, future studies could also compare these tissues in humanized NSG with subclinical and clinical GVHD.

Both humanized NSG mice with subclinical or clinical GVHD were engrafted with similar proportions of human leukocytes as shown indirectly by histology of spleens and directly by flow cytometry of peripheral blood (week 3) and spleens (at end-point). However, the splenic $hCD4^+$:$hCD8^+$ T cell ratios were significantly greater in humanized mice with clinical GVHD compared to mice with subclinical GVHD. This finding is consistent with observations that disease development in humanized NSG mice is mediated by $hCD4^+$ T cells [14,39]. Furthermore, the high $CD4^+$:$CD8^+$ T cell ratios in humanized mice with clinical GVHD parallels with studies in humans, in which high $CD4^+$:$CD8^+$ T cell ratios indicate greater disease severity [40,41]. These observations contrast other findings in humanized NSG mice, where increased $hCD4^+$:$hCD8^+$ T cell ratios correlated with reduced disease severity following IL-21 blockade to prevent GVHD [42]. However, this treatment reduced the number of $hCD4^+$ (and $hCD8^+$) T cells, indicating that the absolute number of $hCD4^+$ T cells may also be important for GVHD development. Additionally, a recent study by Brehm, et al. [43] demonstrated similar $hCD4^+$:$hCD8^+$ T cell ratios in NSG mice and NSG mice deficient in both MHC class I and II, despite MHC class I/II knockout mice showing delayed GVHD development.

Serum hIFN-γ concentrations were significantly increased in humanized NSG mice with clinical GVHD compared to those with subclinical GVHD. There was also a trend of increased hIFN-γ expression in the spleens and livers of mice with clinical GVHD. Reduced serum IFN-γ has been used as a marker to demonstrate a reduction in disease severity in allogeneic [44] and humanized mouse models [23,45] following treatments to prevent GVHD. However, the current study is the first to demonstrate that increased serum hIFN-γ concentrations in humanized mice are associated with clinical GVHD. A recent study by Ehx, et al. [46] confirms our previous findings [23], that $CD8^+$ T cells are the prominent producers of hIFN-γ in NSG mice, but $CD4^+$ T cells have also been shown to produce hIFN-γ [35]. Therefore, it would be of value to determine if blockade or knockdown of hIFN-γ prevents GVHD in humanized NSG mice to directly establish a role for this cytokine in this disease model.

The current study further demonstrated the presence of $hFoxP3^+$ Treg cells in the spleens, livers and small intestines of humanized NSG mice. This data parallels earlier studies that demonstrated the presence of Treg cells in blood, spleens and livers of humanized NSG mice [19]. Collectively, these studies demonstrate that $hFoxP3^+$ Treg cells can traffic to target organs in this humanized mouse model of GVHD. This is important, as Treg cells need to migrate to target organs to interact with effector T cells to promote anti-inflammatory effects and reduce GVHD severity [47]. In the current study there was a trend of increased $FoxP3^+$ Treg cells in the small intestines of mice with clinical GVHD compared to subclinical GVHD. Although this result is contrary to expectations, it may reflect a compensatory attempt to suppress the effector T cells mediating intestinal damage in mice with clinical GVHD. Alternatively, the increased intestinal FoxP3 expression may represent $FoxP3^{lo}$ expressing T cells, which can differentiate to Th17 cells [48], consistent with the hIL-17 expression in the small intestines of mice with clinical GVHD compared to mice with subclinical GVHD. This increased intestinal IL-17 expression is consistent with the role of IL-17 in GVHD development [27]. Moreover, depletion of donor Th17 cells can delay GVHD [28]. However, the role of IL-17 in GVHD is complicated, with IL-17 also showing a protective role in intestinal GVHD [49]. Thus, the increased IL-17 expression in the small intestines of mice with clinical GVHD may reflect increased pathology or a compensatory mechanism to protect against intestinal GVHD in these mice.

In conclusion, the current study identified increases in splenic $hCD4^+$:$hCD8^+$ T cell ratios, serum hIFN-γ concentrations and intestinal hIL-17 in humanized mice with clinical GVHD compared to mice with subclinical GVHD, consistent with observations in human HSCT recipients with GVHD. The cellular and molecular changes identified in the current study could also be used as potential biomarkers in this preclinical model. Furthermore, this data provides insight into GVHD development in this preclinical model, which may aid investigation of potential therapeutics due to the ability to target human cells and investigate human immune responses in these humanized mice.

Acknowledgements

This project was funded by the Illawarra Health and Medical

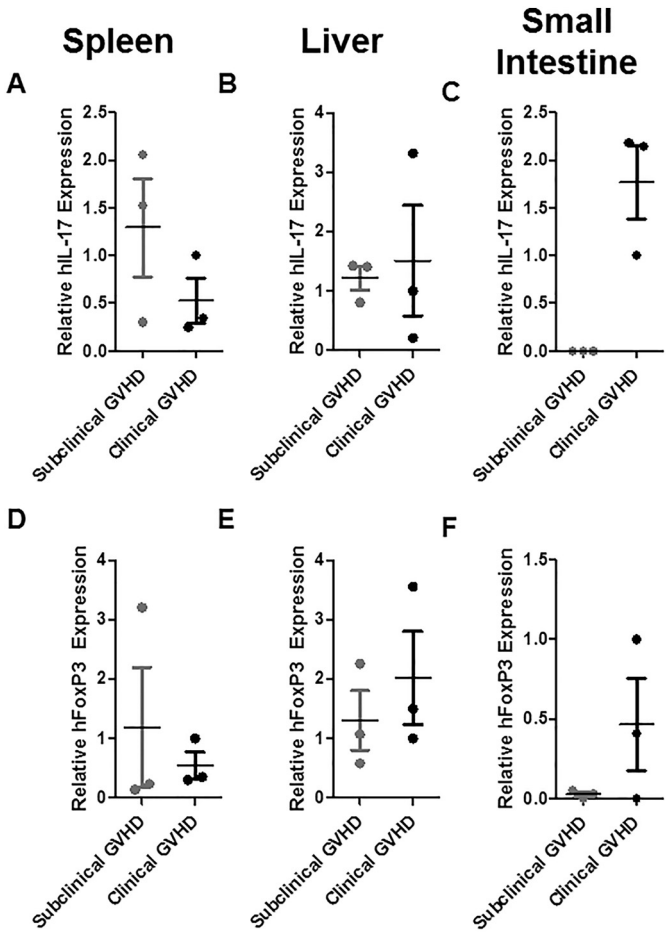

Fig. 5. Humanized mice with clinical GVHD demonstrate increased intestinal hIL-17.
The relative expression of (A-C) hIL-17 and (D-F) hFoxP3 in (A, D) spleens, (B, E) livers and (C, F) small intestines from mice with subclinical and clinical GVHD at end-point were examined by qPCR. Data represents group means ± SEM (n = 3 per group); symbols represent individual mice from two experiments using a single hPBMC donor.

Research Institute and Molecular Horizons (University of Wollongong) and the AMP Tomorrow Fund. We would like to thank the technical staff of the Illawarra Health and Medical Research Institute, and the animal house staff at the Westmead Animal Facility and the University of Wollongong for assistance.

Conflict of interest

The authors declare that they have no conflicts of interest.

Author contributions

N. J. G., L. B., S. R. A., S. I. A., R. S. and D. W. designed and performed the experiments. N. J. G., L. B., S. R. A. analyzed the data. N. J. G. prepared the figures and wrote the manuscript. L. B. and S. R. A reviewed the manuscript. S. I. A. provided mice and reviewed the manuscript. R. S. and D. W. supervised the project, reviewed the data and edited the manuscript.

Reference list

[1] S.Z. Pavletic, D.H. Fowler, Are we making progress in GVHD prophylaxis and treatment? ASH Educ. Program Book 2012 (2012) 251–264.
[2] K.A. Markey, K.P.A. MacDonald, G.R. Hill, The biology of graft-versus-host disease: experimental systems instructing clinical practice, Blood 124 (2014) 354–362.
[3] R.E. Billingham, The biology of graft-versus-host reactions, Harvey Lect. 62 (1965) 21–78.
[4] J.L. Ferrara, R. Levy, N.J. Chao, Pathophysiologic mechanisms of acute graft-vs.-host disease, Biol. Blood Marrow Transplant. 5 (1999) 347–356.
[5] J.L. Ferrara, J.E. Levine, P. Reddy, E. Holler, Graft-versus-host disease, Lancet 373 (2009) 1550–1561.
[6] T. Yi, Y. Chen, L. Wang, et al., Reciprocal differentiation and tissue-specific pathogenesis of Th1, Th2, and Th17 cells in graft-versus-host disease, Blood 114 (2009) 3101–3112.
[7] K.H. Gartlan, K.A. Markey, A. Varelias, et al., Tc17 cells are a proinflammatory, plastic lineage of pathogenic CD8+ T cells that induce GVHD without antileukemic effects, Blood 126 (2015) 1609–1620.
[8] M. Edinger, P. Hoffmann, J. Ermann, K. Drago, C.G. Fathman, S. Strober, R.S. Negrin, CD4+ CD25+ regulatory T cells preserve graft-versus-tumor activity while inhibiting graft-versus-host disease after bone marrow transplantation, Nat. Med. 9 (2003) 1144–1150.
[9] J.J. Auletta, K.R. Cooke, Bone marrow transplantation: new approaches to immunosuppression and management of acute graft-versus-host disease, Curr. Opin. Pediatr. 21 (2009) 30–38.
[10] L.D. Shultz, F. Ishikawa, D.L. Greiner, Humanized mice in translational biomedical research, Nat. Rev. Immunol. 7 (2007) 118–130.
[11] L.D. Shultz, B.L. Lyons, L.M. Burzenski, et al., Human lymphoid and myeloid cell development in NOD/LtSz-scid IL2Rγnull mice engrafted with mobilized human hemopoietic stem cells, J. Immunol. 174 (2005) 6477–6489.
[12] G.C. Bosma, R.P. Custer, M.J. Bosma, A severe combined immunodeficiency mutation in the mouse, Nature 301 (1983) 527–530.
[13] T. Yamauchi, K. Takenaka, S. Urata, et al., Polymorphic *Sirpa* is the genetic determinant for NOD-based mouse lines to achieve efficient human cell engraftment, Blood 121 (2013) 1316–1325.
[14] M.A. King, L. Covassin, M.A. Brehm, et al., Human peripheral blood leucocyte non-obese diabetic-severe combined immunodeficiency interleukin-2 receptor gamma chain gene mouse model of xenogeneic graft-versus-host-like disease and the role of host major histocompatibility complex, Clin. Exp. Immunol. 157 (2009) 104–118.
[15] G.R. Hill, T. Teshima, A. Gerbitz, L. Pan, K.R. Cooke, Y.S. Brinson, J.M. Crawford, J.L.M. Ferrara, Differential roles of IL-1 and TNF-α on graft-versus-host disease and graft versus leukemia, J. Clin. Invest. 104 (1999) 459–467.
[16] A. Busca, F. Locatelli, F. Marmont, C. Ceretto, M. Falda, Recombinant human soluble tumor necrosis factor receptor fusion protein as treatment for steroid refractory graft-versus-host disease following allogeneic hematopoietic stem cell transplantation, Am. J. Hematol. 82 (2007) 45–52.
[17] D.R. Burger, Y. Parker, K. Guinta, D. Lindner, PRO 140 monoclonal antibody to CCR5 prevents acute xenogeneic Graft-Versus-Host Disease in NOD-Scid IL-2Ry^{null} mice, Biol. Blood Marrow Transplant. 24 (2017) 260–266.
[18] D. Green, K. Dhody, Study of PRO 140 for Prophylaxis of Acute GVHD in Patients With AML or MDS Undergoing Allogeneic Stem-Cell Transplant. (GVHD), clinicaltrials.gov/ct2/show/NCT02737306, (2016) , Accessed date: 22 May 2018.
[19] S. Abraham, R. Pahwa, C. Ye, et al., Long-term engraftment of human natural T regulatory cells in NOD/SCID IL2rγcnull mice by expression of human IL-2, PLoS ONE 7 (2012) e51832.
[20] M. Hannon, C. Lechanteur, S. Lucas, et al., Infusion of clinical-grade enriched regulatory T cells delays experimental xenogeneic graft-versus-host disease, Transfusion 54 (2014) 353–363.
[21] J. Heinrichs, D. Bastian, A. Veerapathran, C. Anasetti, B. Betts, X.-Z. Yu, Regulatory T-cell therapy for graft-versus-host disease, J. Immunol. Res. Ther. 1 (2016) 1–14.
[22] C.G. Kanakry, S. Ganguly, M. Zahurak, et al., Aldehyde dehydrogenase expression drives human regulatory T cell resistance to posttransplantation cyclophosphamide, Sci. Transl. Med. 5 (2013) (211ra157-211ra157).
[23] N.J. Geraghty, L. Belfiore, D. Ly, et al., The P2X7 receptor antagonist Brilliant Blue G reduces serum human interferon-γ in a humanized mouse model of graft-versus-host disease, Clin. Exp. Immunol. 190 (2017) 79–95.
[24] K.R. Cooke, L. Kobzik, T.R. Martin, J. Brewer, J. Delmonte Jr., J.M. Crawford, J.L. Ferrara, An experimental model of idiopathic pneumonia syndrome after bone marrow transplantation: I. The roles of minor H antigens and endotoxin, Blood 88 (1996) 3230–3239.
[25] J.L.M. Ferrara, Pathogenesis of acute graft-versus-host disease: cytokines and cellular effectors, J. Hematother. Stem Cell Res. 9 (2000) 299–306.
[26] A.C. Burman, T. Banovic, R.D. Kuns, et al., IFNγ differentially controls the development of idiopathic pneumonia syndrome and GVHD of the gastrointestinal tract, Blood 110 (2007) 1064–1072.
[27] M.J. Carlson, M.L. West, J.M. Coghill, A. Panoskaltsis-Mortari, B.R. Blazar, J.S. Serody, In vitro-differentiated TH17 cells mediate lethal acute graft-versus-host disease with severe cutaneous and pulmonary pathologic manifestations, Blood 113 (2009) 1365–1374.
[28] L.W. Kappel, G.L. Goldberg, C.G. King, et al., IL-17 contributes to CD4-mediated graft-versus-host disease, Blood 113 (2009) 945–952.
[29] E. Dander, A. Balduzzi, G. Zappa, et al., Interleukin-17–producing T-Helper cells as new potential player mediating graft-versus-host disease in patients undergoing allogeneic stem-cell transplantation, Transplantation 88 (2009) 1261–1272.
[30] T. Cao, A. Soto, W. Zhou, W. Wang, S. Eck, M. Walker, G. Harriman, L. Li, Ex vivo expanded human CD4+CD25+Foxp3+ regulatory T cells prevent lethal xenogenic graft versus host disease (GVHD), Cell. Immunol. 258 (2009) 65–71.
[31] P. Trzonkowski, M. Bieniaszewska, J. Juścińska, A. Dobyszuk, A. Krzystyniak, N. Marek, J. Myśliwska, A. Hellmann, First-in-man clinical results of the treatment of patients with graft versus host disease with human ex vivo expanded CD4+CD25+CD127− T regulatory cells, Clin. Immunol. 133 (2009) 22–26.
[32] S. Naserian, M. Leclerc, A. Thiolat, et al., Simple, reproducible, and efficient clinical

grading system for murine models of acute graft-versus-host disease, Front. Immunol. 9 (2018) 10.
[33] G. Vlad, M.B. Stokes, Z. Liu, et al., Suppression of xenogeneic graft-versus-host disease by treatment with immunoglobulin-like transcript 3-Fc, Hum. Immunol. 70 (2009) 663–669.
[34] G. Ehx, G. Fransolet, L. de Leval, et al., Azacytidine prevents experimental xenogeneic graft-versus-host disease without abrogating graft-versus-leukemia effects, OncoImmunology 6 (2017) e1314425.
[35] Y. Kawasaki, K. Sato, H. Hayakawa, et al., Comprehensive analysis of the activation and proliferation kinetics and effector functions of human lymphocytes, and antigen presentation capacity of antigen-presenting cells in xenogeneic graft-versus-host disease, Biol. Blood Marrow Transplant. 24 (2018) 1563–1574.
[36] S. Abraham, J.G. Choi, C. Ye, N. Manjunath, P. Shankar, IL-10 exacerbates xenogeneic GVHD by inducing massive human T cell expansion, Clin. Immunol. 156 (2015) 58–64.
[37] A. Burlion, S. Brunel, N.Y. Petit, D. Olive, G. Marodon, Targeting the human T-cell inducible COStimulator molecule with a monoclonal antibody prevents graft-vs-host disease and preserves graft vs leukemia in a xenograft murine model, Front. Immunol. 8 (2017) 756.
[38] Y. Nakauchi, S. Yamazaki, S.C. Napier, J.-i. Usui, Y. Ota, S. Takahashi, N. Watanabe, H. Nakauchi, Effective treatment against severe graft-versus-host disease with allele-specific anti-HLA monoclonal antibody in a humanized mouse model, Exp. Hematol. 43 (2015) 79–88.
[39] L. Covassin, S. Jangalwe, N. Jouvet, J. Laning, L. Burzenski, L.D. Shultz, M.A. Brehm, Human immune system development and survival of non-obese diabetic (NOD)-scid IL2rγnull (NSG) mice engrafted with human thymus and autologous haematopoietic stem cells, Clin. Exp. Immunol. 174 (2013) 372–388.
[40] P. Huttunen, M. Taskinen, S. Siitonen, U.M. Saarinen-Pihkala, Impact of very early CD4 + /CD8 + T cell counts on the occurrence of acute graft-versus-host disease and NK cell counts on outcome after pediatric allogeneic hematopoietic stem cell transplantation, Pediatr. Blood Cancer 62 (2015) 522–528.
[41] H. Budde, S. Papert, J.H. Maas, H.M. Reichardt, G. Wulf, J. Hasenkamp, J. Riggert, T.J. Legler, Prediction of graft-versus-host disease: a biomarker panel based on lymphocytes and cytokines, Ann. Hematol. 96 (2017) 1127–1133.
[42] K.L. Hippen, C. Bucher, D.K. Schirm, et al., Blocking IL-21 signaling ameliorates xenogeneic GVHD induced by human lymphocytes, Blood 119 (2012) 619–628.
[43] M.A. Brehm, L.L. Kenney, M.V. Wiles, et al., Lack of acute xenogeneic graft- versus-host disease, but retention of T-cell function following engraftment of human peripheral blood mononuclear cells in NSG mice deficient in MHC class I and II expression, FASEB J. 0 (2018) (fj201800636R).
[44] K. Wilhelm, J. Ganesan, T. Müller, et al., Graft-versus-host disease is enhanced by extracellular ATP activating P2X7R, Nat. Med. 16 (2010) 1434–1438.
[45] J. Gregoire-Gauthier, L. Durrieu, A. Duval, et al., Use of immunoglobulins in the prevention of GvHD in a xenogeneic NOD/SCID/γc- mouse model, Bone Marrow Transplant. 47 (2012) 439–450.
[46] G. Ehx, J. Somja, H.J. Warnatz, et al., Xenogeneic graft-versus-host disease in humanized NSG and NSG-HLA-A2/HHD mice, Front. Immunol. 9 (2018) 1943.
[47] V.H. Nguyen, R. Zeiser, D.L. daSilva, D.S. Chang, A. Beilhack, C.H. Contag, R.S. Negrin, In vivo dynamics of regulatory T-cell trafficking and survival predict effective strategies to control graft-versus-host disease following allogeneic transplantation, Blood 109 (2007) 2649–2656.
[48] M. Miyara, Y. Yoshioka, A. Kitoh, et al., Functional delineation and differentiation dynamics of human $CD4^+$ T cells expressing the FoxP3 transcription factor, Immunity 30 (2009) 899–911.
[49] A. Varelias, K.L. Ormerod, M.D. Bunting, et al., Acute graft-versus-host disease is regulated by an IL-17–sensitive microbiome, Blood 129 (2017) 2172–2185.